ACS OMEGA

Open Access

http://pubs.acs.org/journal/acsodf

Article

Theoretical and Experimental Study on the Preparation of High-Viscosity Magnetic Nanofluid by Combined Surfactants

Nuo Chen, Decai Li,* and Shilin Nie

Cite This: *ACS Omega* 2024, 9, 33522−33527

Read Online

ACCESS | Metrics & More | Article Recommendations

ABSTRACT: In this study, the mechanism by which combined surfactants affect the dispersion stability of magnetic nanofluids (MNFs) was improved. Two stable lubricating oil-based magnetic nanofluids with high viscosity and one with low viscosity were prepared by chemical coprecipitation. Erucic acid and octanoic acid were used as the combined surfactants to modify the Fe_3O_4 nanoparticles (MNPs). The size and morphology of the particles were observed using TEM. The rheological properties were tested with a rotational rheometer. The magnetization of the lubricating oil-based magnetic nanofluids was characterized by VSM. The results indicated that the prepared magnetic nanofluids had high viscosity, high magnetism, and good stability. This study provided ideas for the preparation of a high-viscosity magnetic nanofluid. By using combined surfactants, sufficient steric repulsion energy can be provided to counteract the attraction energy of sterically protected nanoparticles, thus achieving a balance of the dispersion stability of MNF.

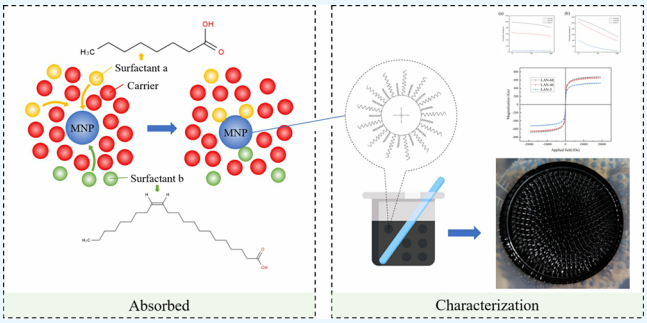

1. INTRODUCTION

As a new type of functional material, magnetic nanofluid has unique properties of both magnetism and fluidity.[1,2] Therefore, it has been widely used in various fields like rotary sealing,[3] lubrication,[4] biomedicine,[5] dampening,[6] tilt measurement sensors,[7] and so on. In order to study the effect of viscosity of magnetic nanofluids on the sealing capability, we need to prepare serial magnetic nanofluids with similar properties but different viscosities.

There are two ways to achieve better enhancement in the viscosity of MNF. One is to couple the magnetic nanoparticles to different additives.[8] The viscosity of Fe_3O_4/Ag MNF increases compared with the traditional Fe_3O_4 MNF.[9] A small amount of tobacco mosaic virus (TMV) added in MNF leads to a significant enhancement in the magnetoviscosity of the cobalt-ferrite ($CoFe_2O_4$)-based magnetic nanofluid.[10] The other way is to increase the viscosity of the carriers. The viscosity values of PAO-60-based MNF were considerably higher than those of PAO-30-based MNF under the same conditions.[11] The viscosity of the silicone-oil-based MNF was lower than that of the fluorine-oil-based MNF at room temperature, precisely because the viscosity of silicone oil (50 cst) was lower than that of fluorine oil (150 cst).[12] The viscosity of ester-based MNF is higher than that of kerosene-based MNF and engine oil-based MNF.[13] In this paper, three kinds of lubricating oils (LAN-5, LAN-46, and LAN-68) were applied as carriers. They have similar properties, but viscosity increases with a higher number. These lubricating oil-based MNFs will meet our requirements. However, it was difficult to prepare a stable MNF using a traditional method (modifying the nanoparticles with one kind of surfactant) when the viscosity comes to the LAN-46 level. Agglomeration would occur as surfactants could not produce enough steric repulsion energy. The initial viscosity of the typical oil-based magnetic nanofluids is in the range of 3−200 mPa s. Therefore, we defined the viscosity above this range as high viscosity.

Previous studies have investigated the effect of unit surfactants on magnetic nanofluids. Various surfactants, e.g., oleic acid, sodium oleate, dodecylamine, and sodium carboxymethylcellulose, are commonly used to enhance dispersibility in carriers.[14] The presence of long-chain molecules adsorbed onto the particle surface can prevent particles from approaching too close to one another. This mechanism is called steric repulsion. Further, for the magnetic nanoparticles in the MNF, the main parameter that determines this mechanism is the surfactant shell thickness, which is proportional to the alkyl chain length. Petrenko, in his study, found that the chain length in LA (C12) was insufficient to

Received: February 1, 2024
Revised: April 1, 2024
Accepted: April 2, 2024
Published: July 22, 2024

provide such stabilization in nonpolar solvent decahydronaphthalene-based MNF he prepared.[15,16] Nagornyi used the small-angle neutron scattering method to investigate the structures of concentrated magnetic nanofluids based on water and stabilized by sodium oleate (SO) or dodecylbenzenesulfonic acid (DBSA). He found that not only the number of free surfactant molecules in solutions but also the surfactant−MNP and surfactant−carrier interactions affect the stabilization mechanism in the MNF.[17,18] In the research of preparing an aqueous magnetic nanofluid, the bilayer surfactant structure was proposed.[19,20] Different kinds of stable aqueous MNF produced various saturated and unsaturated fatty acids as primary and secondary surfactants.[21,22] The inner layer covers the surface of the superparamagnetic core as a monolayer, with the hydrocarbon tail extending out. The outer layer physically adsorbed on the inner layer.[23] Furthermore, γ-irradiation can be effective in polymerizing olefin-terminated surfactant bilayer coatings on magnetite nanoparticles.[24] However, this method can only work in an aqueous medium because these modified particles are hydrophilic. Therefore, there is still no specific theoretical and experimental study on the dispersion stability of oil-based MNF with combined surfactants adsorbed onto the particles.

In this paper, the improved mechanism by which combined surfactants affect the dispersion stability of magnetic nanofluids was presented. Accordingly, erucic acid and octanoic acid were used as the combined surfactants to modify the Fe_3O_4 nanoparticles. Then, materials and the characterization methods for MNF preparation were proposed. The rest of the paper is organized as follows: Section 4 discusses the experimental results, and Section 5 summarizes the conclusions and future works.

2. DISPERSION STABILITY MECHANISM OF COMBINED SURFACTANTS

2.1. Attraction Energy. Dispersion stability depends on the balance between various forms of energy (attractive and repulsive energies) and thermal energy to avoid agglomeration over a period of time.[25] In magnetic nanofluids, the permanently magnetized particles will approach each other because of the magnetic and van der Waals attractive energies. At the same time, the long-chain molecules adsorbed on the particle surface will produce steric repulsion energy to prevent this phenomenon. Agglomeration occurs in a magnetic nanofluid if the average thermal energy exceeds the sum of the total interactions (barrier energy).[26] These thermal and attraction energies per particle are

thermal energy: $E_T = kT$

magnetic attractive energy: $E_{dd} = -\dfrac{\pi\mu_0 M^2 d_p^3}{72\left(1+\frac{d_s}{d_p}\right)^3}$

van der Waals attractive energy: $E_f = \dfrac{A}{6}\left[\dfrac{2}{l^2+4l} + \dfrac{2}{(l+2)^2} + \ln\dfrac{l^2+4l}{(l+2)^2}\right]$

where k is the Boltzmann constant and equals 1.38×10^{-23} N m K^{-1}, T is the absolute temperature in degrees Kelvin, μ_0 is the permeability of free space and has the value $4\pi \times 10^{-7}$ H m, volume $V = \pi {d_p}^3/6$ m^3 for a spherical particle of diameter d_p, d_s is the distance between two particles' surfaces, and $l = 2d_s/d_p$, where A is the Hamaker constant equaling $(1-3) \times 10^{-19}$ N m.

2.2. Steric Repulsion Energy. Mackor treated steric repulsion as the statistical mechanics of a rigid rod attached onto a universal hinge.[27] It was assumed that the "head" polar group of the adsorbed molecule is dilute at the surface, so that the "tail" rod can adopt a hemispherical orientation under the influence of thermal motion. Based on this, we developed a double-chained model to reveal the effect of combined surfactants on the dispersion stability of the magnetic nanofluid (see Figure 1). When two particles approach each other and are in close proximity, the surface-adsorbed long-chain molecule layers will be compressed like elastic bumpers. With different particle distances and chain lengths, we can calculate the repulsion energy using this model.

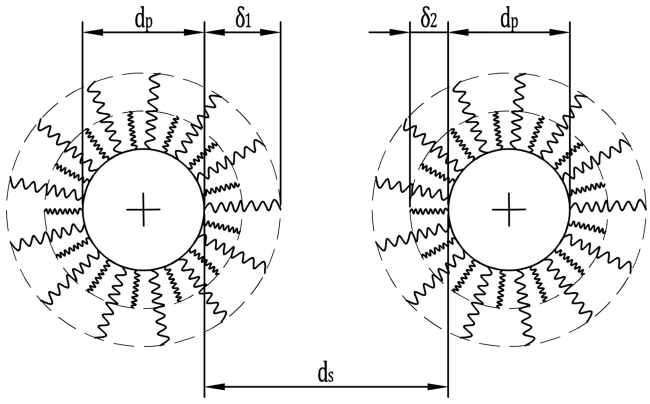

Figure 1. Geometric illustration of the double-chained model.

The lengths of the two surfactant chains are δ_1 and δ_2, respectively, and $\delta_1 > \delta_2$. As the distance reduces, the relative long-chain molecules will get in touch first. Then, the relative long and relative short molecules, and finally the relative short molecules will compress each other. Accordingly, we can obtain the expression for the repulsive energy per unit area of the surface, which is

$$E_r = \sum_{i,j=1}^{2} \pi d_p^2 p_{ij} \xi_i k_0 T\left[1 - \frac{\overline{d}_{s_i}}{2\overline{\delta}_i} - \frac{1+(\overline{d}_{s_i}/2)}{\overline{\delta}_i}\ln\frac{1+\overline{\delta}_i}{1+(\overline{d}_{s_i}/2)}\right]$$

where $\overline{d}_{s_i} = 2d_{s_i}/d_p$, $d_{s_i} = d_s^*(\delta_i/\sum\delta_i)$, $\overline{\delta}_i = 2\delta_i/d_p$, p_{ij} is the proportion of surfactant molecules i compressed by surfactant molecules j, and ξ is the surface concentration of adsorbed molecules.

2.3. Cage Effect. As we can learn from the expression, in addition to the surfactant shell thickness, the surface concentration of adsorbed molecules is also a main parameter that determines the steric repulsion. Usually, the preparation is pictured as the behavior of isolated molecules in which the carrier is treated as a passive support. However, the nature of the carrier can actually influence the rate and sequence of the reaction.[20] Hence, it is more accurate to describe the surfactant molecules and magnetic nanoparticles in the carrier as encapsulated particles in the preparation of MNFs. The encapsulated particles must diffuse from their carrier cages to

https://doi.org/10.1021/acsomega.4c01060
ACS Omega 2024, 9, 33522−33527

interact with other particles. This mechanism is called cage effect (see Figure 2). Further, this effect is enhanced as the

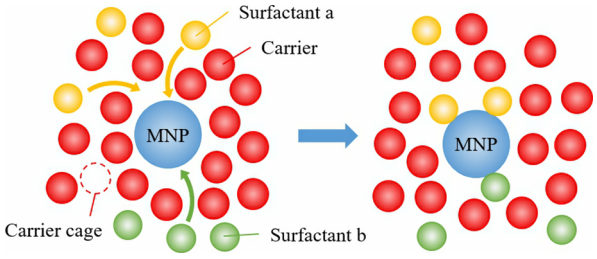

Figure 2. Free surfactant molecules in carriers can diffuse out from their cages to react with a particle within another cage.

viscosity of the carrier increases.[21] It is more difficult for surfactants to diffuse and then get absorbed onto the MNPs as more energy is needed, which leads to a decrease in the surface concentration. This is one of the reasons why the preparation of high-viscosity magnetic nanofluids is a hard nut to crack.

2.4. Net Interaction Curve. It is the algebraic sum of the magnetic attractive energy, van der Waals attractive energy, and steric repulsion energy that is decisive for determining the dispersion stability of the particle suspensions. Figure 3

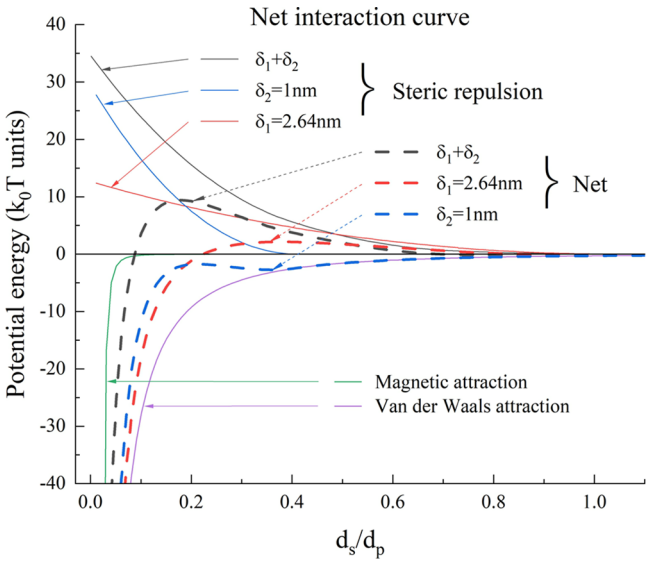

Figure 3. Attraction energy and repulsion energy of the particle suspensions.

illustrates this behavior using MATLAB, where we take the attraction energy as negative and the repulsion energy as positive. The abscissa, or x-coordinate, may represent the dimensionless distance between two particle surfaces (i.e., d_s/d_p). On the ordinate, or y-coordinate, is the dimensionless potential energy as the ratio of attractive or repulsive energy to thermal energy (k_0T).

Typical values of parameters are T = 298 K and $A = 2 \times 10^{-19}$ N m. Based on the characterization of MNPs we have made, the diameter of the particle is d_p = 10 nm, and the saturation magnetization is M = 5800 Gs. Considering the double-chain model we presented, two surfactants with chain lengths of δ_1 = 2.64 nm and δ_2 = 1 nm are included in the calculation. Respectively, the surface concentration is $\xi_1 = 0.2 \times 10^{18}/m^2$ and $\xi_2 = 1 \times 10^{18}/m^2$. The black curves represent the situation where two surfactant molecules are absorbed onto the particle surfaces. The blue curves indicate the isolated absorption of relative long molecules and the red ones for relative short molecules. The green one means magnetic attraction energy, and the purple one is van der Waals attractive energy.

We can learn that when two particles approach each other, the repulsive energy increases, which then leads to an increase in the net interaction energy. At a specific distance, the algebraic sum of these energies reaches the maximum value and creates an energy barrier. Different results emerge in different cases. Case 1 is where just relatively short molecules are absorbed in isolation, and the repulsive energy generated by the surfactants is too weak to overpower the attractive energy. The occurrence of agglomeration is taken for granted. In case 2, just the relatively long molecules are absorbed in isolation, and the energy barrier becomes positive. However, the barrier is just about $2k_0T$, which is still not strong enough to keep the whole system stable for a long period. Case 3 is the double-absorbed model with an energy barrier of more than $10k_0T$. As this barrier energy exceeds the average thermal energy of a particle by an order of magnitude, statistically, few particles will cross the barrier, and the rate of agglomeration should be negligible. From these curves, we can have a very clear understanding of the key role of combined surfactants in the preparation of high-viscosity magnetic nanofluids. Furthermore, the interactions between surfactants we ignored this time may affect the absorption and should be taken into consideration in a future study.

3. EXPERIMENTAL SECTION

3.1. Materials. The chemicals used in this work were all analytical grade, without further purification. Ferric chloride ($FeCl_3$) was purchased from Shanghai Titan Scientific Co., Ltd., ferrous chloride tetrahydrate ($FeCl_2{\cdot}4H_2O$) from Damao Chemical Reagent Factory, and ammonia solution ($NH_3{\cdot}H_2O$) from Xilong Scientific Co., Ltd. Erucic acid and octanoic acid were provided by Meryer (Shanghai) Biochemical Technology Co., Ltd. Three kinds of lubricating oil (LAN-5, LAN-46, and LAN-68) were applied in our experiment as carriers and supplied by Mojiezuo Petrochemical (Shanghai) Co., Ltd. Deionized water was used throughout the experiments.

3.2. Preparation of Lubricating Oil-Based Magnetic Nanofluids. The lubricating oil-based magnetic nanofluids tested in this study can be prepared using the process shown in Figure 4. Fe_3O_4 MNPs were synthesized by the coprecipitation method, and the reaction process was: $Fe^{2+} + 2Fe^{3+} + 8OH^- \rightarrow Fe_3O_4 + 4H_2O$. According to the mole ratio of 1:2, a mixture of ferric chloride ($FeCl_3$) and ferrous chloride tetrahydrate ($FeCl_2{\cdot}4H_2O$) was dissolved into deionized water and placed into a 45 °C thermostat water bath. Under vigorous stirring, enough ammonia solution was added. After 45 min, the solution was washed with deionized water and put on a magnet several times until the supernatant pH reduced to about 7. By this process, the Fe_3O_4 MNPs were isolated. To further modify the MNPs, surfactants were used. First, these obtained MNPs were dispersed in a specific kind of lubricating oil. Then, a mixture of erucic acid and octanoic acid was added into it. A 2 h 80 °C thermostat water bath along with vigorous stirring was used to ensure the MNPs were fully covered by the surfactants. Finally, the solution was put on a strong magnet for 24 h to precipitate the possible large particles, and after that, a stable lubricating oil-based magnetic nanofluid was

https://doi.org/10.1021/acsomega.4c01060
ACS Omega 2024, 9, 33522−33527

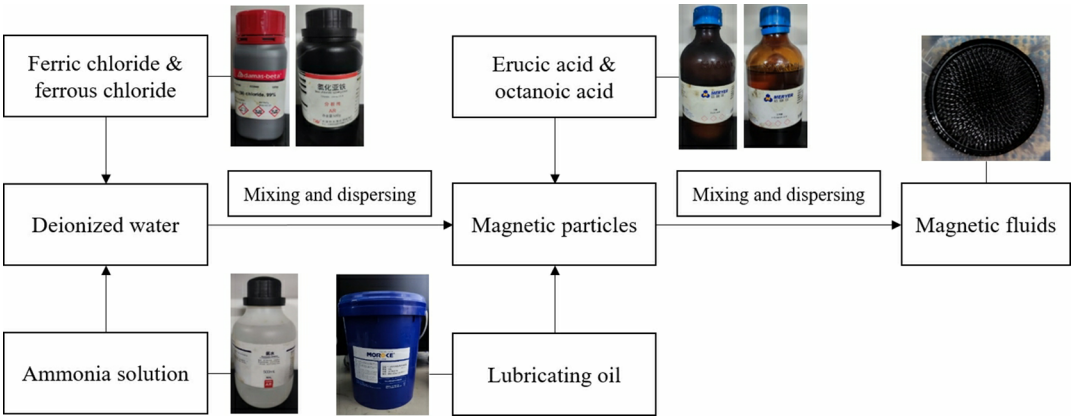

Figure 4. Process of preparing lubricating oil-based magnetic nanofluids.

obtained. Finally, we obtained one kind of low-viscosity oil-based MNF (LAN 5 based) and two kinds of high-viscosity oil-based MNFs (LAN 46-based and LAN 68-based).

In addition, we also tried to prepare LAN-46-based MNF in the conventional method using just one single type of surfactant to modify the nanoparticles, and agglomeration and segregation occurred (see Figure 5).

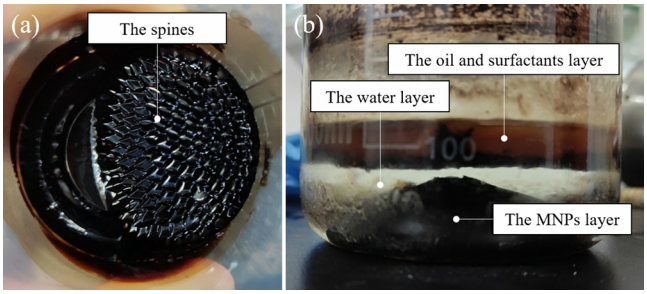

Figure 5. (a) Successfully prepared MNF. (b) Agglomeration and separation.

3.3. Characterization Methods. The magnetic fluids were identified by a transmission electron microscope (NEC, JEM-2010), a rotational rheometer (Anton Paar, MCR-302), and a vibrating sample magnetometer (VSM, Microsense, EZ-8).

4. RESULTS AND DISCUSSION

4.1. TEM Results of Magnetic Particles. Figure 6 shows the TEM images of the prepared MNPs. As we can see, the particles were spherical, and the average diameter was about 10 nm, which was within the range of particle size of stable colloids.[27] The modification of surfactants did not result in the agglomeration of MNPs which was in accordance with the macroscopic view of the MNFs.

4.2. Rheological Properties of MNFs. Figure 7 shows the variations of the viscosity of the prepared MNFs under different magnetic fields as the temperature was kept at 25 °C. There are three curves of the samples including LAN-5, LAN-46, and LAN-68 lubricating oil-based MNFs in each graph. Figure 7a reveals that the viscosity of all the prepared MNFs remained steady with the increasing shear rate in the absence of a magnetic field. Newtonian fluid characteristics were observed which were similar to the behavior of the carrier fluid. When the static magnetic field was applied to the MNFs, the viscosity rose sharply because the particle chains composed of MNPs were formed.[28−31] The particle chains could enhance the capacity for the resistance of shear forces. However, as the shear rate rose, the chains would be destroyed, and MNPs could rearrange their orientation. In this situation, Figure 7b reflects the downward trend of viscosity with an increasing shear rate, indicating the shear-thinning nature of the MNFs.

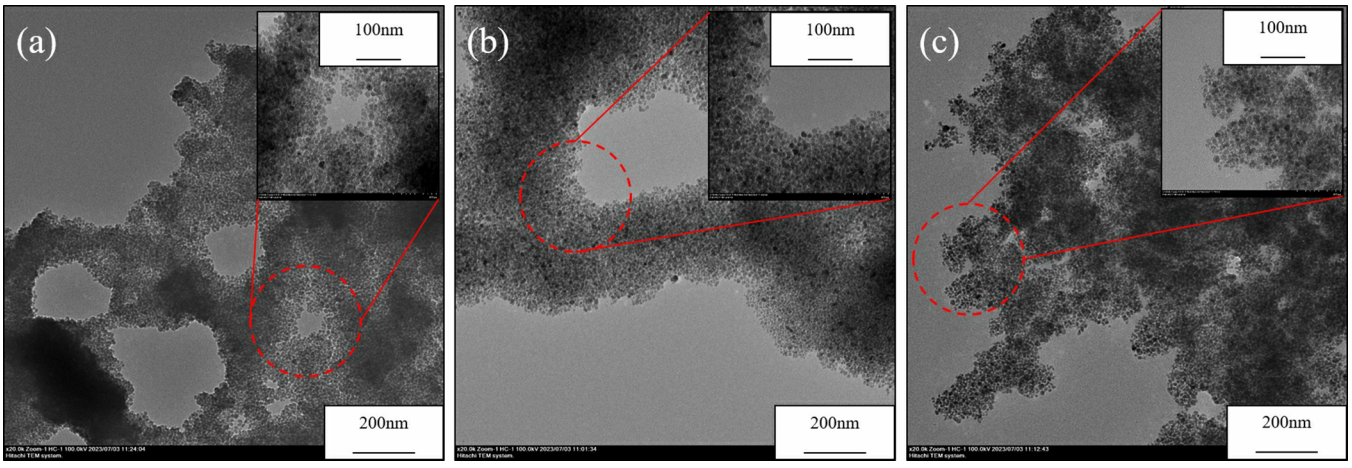

Figure 6. TEM images of prepared MNPs: (a) LAN-5; (b) LAN-46; and (c) LAN-68.

https://doi.org/10.1021/acsomega.4c01060
ACS Omega 2024, 9, 33522−33527

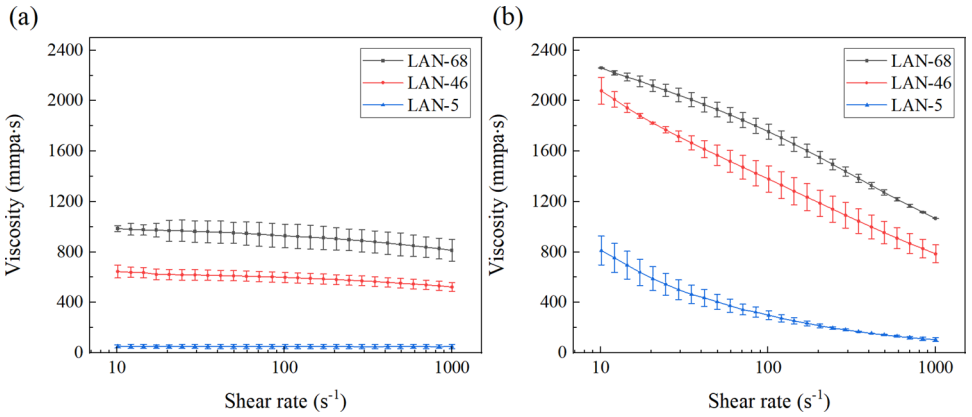

Figure 7. Magnetoviscosity curves of the prepared MNFs (a) at 0 T and (b) at 0.32 T.

4.3. Magnetic Properties of MNFs. Figure 8 shows the hysteresis loops of the prepared MNFs, and similar magnetization curve shapes of all samples were observed. Nearly immeasurable coercivity and remanence revealed the superparamagnetic properties of the prepared MNFs, which were in line with the theory. However, the saturated magnetization of LAN-5-based MNF, LAN-46-based MNF, and LAN-68-based MNF was 521.53, 650.37, and 678.07 Gs, respectively.

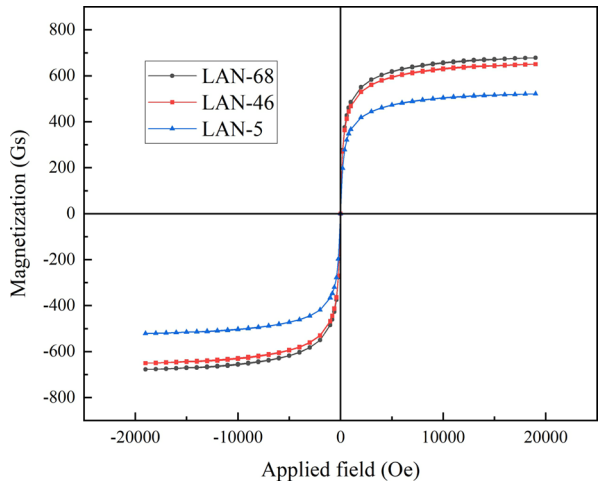

Figure 8. Magnetic hysteresis curves of the prepared MNFs.

5. CONCLUSIONS

In our study, we improved the mechanism of the effect of combined surfactants on the dispersion stability of the magnetic nanofluid. Erucic acid and octanoic acid were used to prepare stable lubricating oil-based magnetic nanofluids with high viscosity. The good appearance of the prepared MNFs and the following characterized results indicated that this preparation method did work in both low-viscosity and high-viscosity carrier fluids. The average particle size of the MNPs was about 10 nm. The viscosity of LAN-5-based MNF, LAN-46-based MNF, and LAN-68-based MNF at the temperature of 25 °C, magnetic field of 0.32 T, and shear rate of 10^{-1} s was 812.16, 2078.7, and 2260.0 mPa s, respectively. The saturated magnetization was 521.53, 650.37, and 678.07 Gs, respectively.

AUTHOR INFORMATION

Corresponding Author

Decai Li − *Tsinghua University State Key Laboratory of Tribology, Beijing 100084, China*; Email: lidecai@mail.tsinghua.edu.cn

Authors

Nuo Chen − *Tsinghua University State Key Laboratory of Tribology, Beijing 100084, China*; orcid.org/0009-0008-0031-150X

Shilin Nie − *Tsinghua University State Key Laboratory of Tribology, Beijing 100084, China*

Complete contact information is available at: https://pubs.acs.org/10.1021/acsomega.4c01060

Notes

The authors declare no competing financial interest.

ACKNOWLEDGMENTS

The work was supported by the National Key R&D Program of China (grant no. 2020YFB2006900) and National Natural Science Foundation of China (grant nos. 51927810, U1837206, and 51735006).

REFERENCES

(1) Odenbach, S. Ferrofluids - magnetically controlled suspensions. *Colloids Surf., A* **2003**, *217* (1−3), 171−178.

(2) Kadau, H.; Schmitt, M.; Wenzel, M.; Wink, C.; Maier, T.; Ferrier-Barbut, I.; Pfau, T. Observing the Rosensweig instability of a quantum ferrofluid. *Nature* **2016**, *530* (7589), 194.

(3) Li, D. C.; Li, Y. W.; Li, Z. X.; Wang, Y. M. Theory analyses and applications of magnetic fluids in sealing. *Friction* **2023**, *11* (10), 1771−1793.

(4) Yu, J.; Li, D. C.; Li, S. B.; Xiang, Z. Y.; He, Z. D.; Shang, J.; Li, R. W. Electromagnetic vibration energy harvester using magnetic fluid as lubricant and liquid spring. *Energy Convers. Manage.* **2023**, *286*, No. 117030.

(5) Liangruksa, M.; Ganguly, R.; Puri, I. K. Parametric investigation of heating due to magnetic fluid hyperthermia in a tumor with blood perfusion. *J. Magn. Magn. Mater.* **2011**, *323* (6), 708−716.

(6) Li, Y. W.; Han, P. D.; Li, D. C.; Chen, S. Y.; Wang, Y. M. Typical dampers and energy harvesters based on characteristics of ferrofluids. *Friction* **2023**, *11* (2), 165−186.

(7) Medvegy, T.; Molnar, A.; Molnar, G.; Gugolya, Z. Analysis of a ferrofluid core differential transformer tilt measurement sensor. *J. Magn. Magn. Mater.* **2017**, *428*, 189−193.

https://doi.org/10.1021/acsomega.4c01060
ACS Omega 2024, 9, 33522−33527

(8) Felicia, L. J.; Vinod, S.; Philip, J. Recent Advances in Magnetorheology of Ferrofluids (Magnetic Nanofluids)—A Critical Review. *Journal of Nanofluids* **2016**, *5* (1), 1−22.
(9) Qianhui, C.; Zhili, Z.; Nannan, D.; Guobao, Z.; Decai, L. Study on the Fluidity Experiments of Engine Oil-Based Magnetic Fluid with Fe3O4/Ag Nanoparticles. *IOP Conf. Ser.: Mater. Sci. Eng.* **2019**, *678*, No. 012145.
(10) Wu, Z. Y.; Mueller, A.; Degenhard, S.; Ruff, S. E.; Geiger, F.; Bittner, A. M.; Wege, C.; Krill, C. E. Enhancing the Magnetoviscosity of Ferrofluids by the Addition of Biological Nanotubes. *ACS Nano* **2010**, *4* (8), 4531−4538.
(11) Kim, J. H.; Park, K. B. Properties of Polyalphaolefin-Based Ferrofluids. *Journal of Magnetics* **2015**, *20* (4), 371−376.
(12) Kim, J.-H.; Park, G.-B.; Kim, K.-S. Preparation and Characterization of Silicone and Fluorine-Oil-Based Ferrofluids [research-article]. *Compos. Res.* **2017**, *30* (1), 41−45.
(13) Cui, H. C.; Li, D. C. Preparation and Property Research of Perfluoropolyether Oil-Based Ferrofluid. *Journal of Superconductivity and Novel Magnetism* **2018**, *31* (11), 3607−3624.
(14) Sharifi, I.; Shokrollahi, H.; Amiri, S. Ferrite-based magnetic nanofluids used in hyperthermia applications. *J. Magn. Magn. Mater.* **2012**, *324* (6), 903−915.
(15) Petrenko, V. I.; Avdeev, M. V.; Bulavin, L. A.; Almasy, L.; Grigoryeva, N. A.; Aksenov, V. L. Effect of surfactant excess on the stability of low-polarity ferrofluids probed by small-angle neutron scattering. *Crystallography Reports* **2016**, *61* (1), 121−125.
(16) Aksenov, V. L.; Avdeev, M. V.; Shulenina, A. V.; Zubavichus, Y. V.; Veligzhanin, A. A.; Rosta, L.; Vekas, L. Neutron and Synchrotron Radiation Scattering by Nonpolar Magnetic Fluids. *Crystallogr. Rep.* **2011**, *56* (5), 792−801.
(17) Nagornyi, A. V.; Socoliuc, V.; Petrenko, V. I.; Almasy, L.; Ivankov, O. I.; Avdeev, M. V.; Vekas, L. Structural characterization of concentrated aqueous ferrofluids. *J. Magn. Magn. Mater.* **2020**, *501*, No. 166445.
(18) Petrenko, V. I.; Artykulnyi, O. P.; Bulavin, L. A.; Almasy, L.; Garamus, V. M.; Ivankov, O. I.; Avdeev, M. V. On the impact of surfactant type on the structure of aqueous ferrofluids. *Colloids Surf., A* **2018**, *541*, 222−226.
(19) Shimoiizaka, J.; Nakatsuka, K.; Fujita, T.; Kounosu, A. Sink-Float Separators Using Permanent-Magnets and Water Based Magnetic Fluid. *Ieee Transactions on Magnetics* **1980**, *16* (2), 368−371.
(20) Shen, L. F.; Laibinis, P. E.; Hatton, T. A. Bilayer surfactant stabilized magnetic fluids: Synthesis and interactions at interfaces. *Langmuir* **1999**, *15* (2), 447−453.
(21) Wooding, A.; Kilner, M.; Lambrick, D. B. Studies of the Double Surfactant Layer Stabilization of Water-Based Magnetic Fluids. *J. Colloid Interface Sci.* **1991**, *144* (1), 236−242.
(22) Chen, M. J.; Shen, H.; Li, X.; Liu, H. F. Facile synthesis of oil-soluble Fe3O4 nanoparticles based on a phase transfer mechanism. *Appl. Surf. Sci.* **2014**, *307*, 306−310.
(23) Acar, H. Y. C.; Garaas, R. S.; Syud, F.; Bonitatebus, P.; Kulkarni, A. M. Superparamagnetic nanoparticles stabilized by polymerized PEGylated coatings. *J. Magn. Magn. Mater.* **2005**, *293* (1), 1−7.
(24) Shen, L. F.; Stachowiak, A.; Hatton, T. A.; Laibinis, P. E. Polymerization of olefin-terminated surfactant bilayers on magnetic fluid nanoparticles. *Langmuir* **2000**, *16* (25), 9907−9911.
(25) Yu, F.; Chen, Y. Y.; Liang, X. B.; Xu, J. L.; Lee, C. S.; Liang, Q.; Tao, P.; Deng, T. Dispersion stability of thermal nanofluids. *Progress in Natural Science-Materials International* **2017**, *27* (5), 531−542.
(26) Li, J.; Huang, Y.; Liu, X. D.; Lin, Y. Q.; Bai, L.; Li, Q. Effect of aggregates on the magnetization property of ferrofluids: A model of gaslike compression. *Sci. Technol. Adv. Mater.* **2007**, *8* (6), 448−454.
(27) Mackor, E. L. A Theoretical Approach of the Colloid-Chemical Stability of Dispersions in Hydrocarbons. *Journal of Colloid Science* **1951**, *6* (5), 492−495.
(28) Carey, F. A.; Sundberg, R. J. *Advanced organic chemistry: part A: structure and mechanisms*; Springer Science & Business Media: 2007.
(29) Braden, D. A.; Parrack, E. E.; Tyler, D. R. Solvent cage effects. I. Effect of radical mass and size on radical cage pair recombination efficiency. II. Is geminate recombination of polar radicals sensitive to solvent polarity? *Coord. Chem. Rev.* **2001**, *211* (1), 279−294.
(30) Rosensweig, R. E. *Ferrohydrodynamics*; Courier Corporation: 2013.
(31) Li, Z. K.; Li, D. C.; Chen, Y. B. Study on the yielding behaviors of ferrofluids: a very shear thinning phenomenon. *Soft Matter* **2020**, *16* (35), 8202−8212.

https://doi.org/10.1021/acsomega.4c01060
ACS Omega 2024, 9, 33522−33527